INSTITUTE OF PHYSICS PUBLISHING PHYSICS IN MEDICINE AND BIOLOGY

Phys. Med. Biol. **48** (2003) 587–598 PII: S0031-9155(03)57158-5

Synchronized moving aperture radiation therapy (SMART): average tumour trajectory for lung patients

Toni Neicu[1], **Hiroki Shirato**[2], **Yvette Seppenwoolde**[3] **and Steve B Jiang**[1]

[1] Department of Radiation Oncology, Massachusetts General Hospital and Harvard Medical School, Boston, MA, USA
[2] Department of Radiation Medicine, Hokkaido University School of Medicine, Sapporo, Japan
[3] Department of Radiotherapy, The Netherlands Cancer Institute/Antoni van Leeuwenhoek Hospital, Amsterdam, The Netherlands

Received 5 December 2002
Published 18 February 2003
Online at stacks.iop.org/PMB/48/587

Abstract

Synchronized moving aperture radiation therapy (SMART) is a new technique for treating mobile tumours under development at Massachusetts General Hospital (MGH). The basic idea of SMART is to synchronize the moving radiation beam aperture formed by a dynamic multileaf collimator (DMLC) with the tumour motion induced by respiration. SMART is based on the concept of the average tumour trajectory (ATT) exhibited by a tumour during respiration. During the treatment simulation stage, tumour motion is measured and the ATT is derived. Then, the original IMRT MLC leaf sequence is modified using the ATT to compensate for tumour motion. During treatment, the tumour motion is monitored. The treatment starts when leaf motion and tumour motion are synchronized at a specific breathing phase. The treatment will halt when the tumour drifts away from the ATT and will resume when the synchronization between tumour motion and radiation beam is re-established. In this paper, we present a method to derive the ATT from measured tumour trajectory data. We also investigate the validity of the ATT concept for lung tumours during normal breathing. The lung tumour trajectory data were acquired during actual radiotherapy sessions using a real-time tumour-tracking system. SMART treatment is simulated by assuming that the radiation beam follows the derived ATT and the tumour follows the measured trajectory. In simulation, the treatment starts at exhale phase. The duty cycle of SMART delivery was calculated for various treatment times and gating thresholds, as well as for various exhale phases where the treatment begins. The simulation results show that in the case of free breathing, for 4 out of 11 lung datasets with tumour motion greater than 1 cm from peak to peak, the error in tumour tracking can be controlled to within a couple of millimetres while maintaining a reasonable delivery efficiency. That is to say, without any breath coaching/control, the ATT is a valid concept for some lung tumours. However, to make SMART an efficient technique in general, it is found that breath coaching techniques are required.

1. Introduction

Tumour motion caused by patient breathing poses a challenging problem for chest and abdominal radiation therapy treatments. Several methods have been proposed to solve this problem. The conventional solution is to expand the planning target volume to ensure that the entire clinical target volume will receive the prescribed dose. However, the unintended consequence of target expansion is the delivery of high dose to adjacent critical structures. This can lead to serious side effects, resulting in an inability to escalate tumour dose. Gating of the radiation beam with the breathing cycle (Suit *et al* 1988, Ohara *et al* 1989, Kubo and Hill 1996, Ramsey *et al* 1999a, 1999b, Kubo *et al* 2000, Kubo and Wang 2000, Minohara *et al* 2000, Shirato *et al* 2000, Vedam *et al* 2001) and the breath-hold techniques (Hanley *et al* 1999, Wong *et al* 1999, Rosenzweig *et al* 2000, Mah *et al* 2000, Stromberg *et al* 2000) represent improved methods that lead to a reduction of the internal tumour margins in the planning target volume. The main weakness of the breath-hold technique is that it may not be well tolerated by general lung cancer patients (Kubo *et al* 2000).

When the gating technique is used, radiation is delivered only when the tumour reaches a pre-selected position that is detected either directly or indirectly. Direct detection can be achieved by on-line diagnostic x-ray imaging of internal fiducial markers (Shirato *et al* 2000, Seppenwoolde *et al* 2002). Tumour position can also be detected indirectly by monitoring surface surrogates or lung air flow during breathing and relating them to the position of the tumour (Kubo and Hill 1996, Kubo *et al* 2000, Minohara *et al* 2000, Ford *et al* 2002, Ozhasoglu and Murphy 2002). However, there is an inherent conflict between the desire to increase gating efficiency and at the same time reduce the gating window size. To increase the duty cycle, the gating window must be enlarged, resulting in the irradiation of more normal tissue. This problem is more severe in intensity modulated radiation therapy (IMRT) where longer treatment time is usually required. An alternative technique is to synchronize the radiation beam with the tumour motion. This was first implemented in a robotic radiosurgery system (Adler *et al* 1999, Ozhasoglu *et al* 2000, Schweikard *et al* 2000, Murphy *et al* 2002). For linac-based radiotherapy, tumour motion can be compensated for with dynamic multileaf collimator (DMLC), as recently proposed independently by Keall *et al* (2001) and by our group.

The implementation of the tumour motion synchronization technique at Massachusetts General Hospital (MGH) is called synchronized moving aperture radiation therapy (SMART). Our goal is to improve the effectiveness and efficiency of IMRT for treating mobile tumours in the thorax and abdomen. At treatment simulation/planning stage, the tumour motion can be measured on a simulator or a linac-mounted imaging system, and the average tumour trajectory (ATT) is then derived. Using the ATT, tumour motion can be incorporated into the IMRT leaf sequence either during or after the process of leaf sequencing. At treatment delivery stage, respiratory surrogates or implant markers are monitored and used to synchronize the treatment with tumour motion. The beam moves according to the ATT and is turned off when the tumour's position differs from the average trajectory. The treatment is resumed when the radiation beam motion and tumour motion are re-synchronized. The beam is turned on and moves along the ATT again. Therefore, SMART can be thought of as a combination of respiratory gating and DMLC tumour tracking.

Two key requirements for successfully using SMART in clinical practice are precise and real-time detection of the tumour position during simulation/treatment, and a regular tumour motion pattern. To fulfil the first requirement, an integrated radiotherapy imaging system (IRIS) is currently being developed at MGH. The work reported in this paper is a theoretical investigation which deals with two questions related to the second requirement: (1) how to

derive the ATT from the measured tumour trajectory data, and (2) is ATT a well-defined concept for lung cancer patients breathing freely?

2. Method and materials

2.1. Data acquisition

The patient tumour trajectory data used in the present study was acquired by a real-time tumour-tracking system at Hokkaido University (Shirato *et al* 2000). The system is capable of tracking the 3D position of a 2.0 mm diameter gold marker in the lung at 30 Hz. The system consists of four sets of diagnostic x-ray imaging systems which are mounted on the floor and ceiling in the treatment room. During the treatment, at least two x-ray tube-imagers are unobstructed by the linac gantry and can provide a pair of orthogonal images. Both images are digitized to 1024×1024 pixels with 8 bits per pixel, and are fed to an image processor unit that consists of two image acquisition units, two image recognition units and a central processor unit (CPU).

The tracking of the implanted gold marker in the digital images is performed by means of a template matching algorithm using special hardware. The tracking result is the 3D coordinates of the marker, i.e., $x(t)$ (left–right direction), $y(t)$ (cranial–caudal direction) and $z(t)$ (anterior–posterior direction). The marker position is considered to correlate well with the tumour position. The 3D coordinates of the marker are recorded every $1/30$ s and used to gate the linac. The accuracy of the real-time tracking system was found to be better than 1.5 mm for moving targets up to a speed of 40 mm s^{-1}.

Forty-one datasets with average recording length of 150 s were measured with this real-time tumour-tracking system and used for the present study. These data belong to 20 patients and 21 tumours. Due to the small size of the data pool, each dataset will be treated independently, as if it belonged to a different patient.

2.2. Deriving average tumour trajectory (ATT)

A method has been developed to derive the ATT from the measured 3D tumour trajectory data ($[x(t), y(t), z(t)]$) and has been applied to datasets with a maximum peak-to-peak tumour motion greater than 1 cm. For tumours with small motion, there is less need to apply any motion mitigation techniques such as respiratory gating or SMART.

For each dataset, a smoothing procedure is first applied to remove the data noise due to inherent inaccuracies in the tumour position measurement. We used a 30 point median filter for all the datasets. Based on the characteristics of the real-time tumour-tracking system signal, we found that this filter smoothed enough noise, without losing the tumour location information.

The velocity of the tumour along its 3D trajectory is calculated as a function of time

$$v(t) = \left\| \frac{\mathrm{d}\vec{r}(t)}{\mathrm{d}t} \right\|$$

where

$$\vec{r}(t) = x(t)\vec{e}_x + y(t)\vec{e}_y + z(t)\vec{e}_z.$$

The minima of the velocity $v(t)$ curve are identified and assigned to corresponding inhale or exhale breathing phases. Therefore, each breathing cycle can be identified from the measured trajectory data. Then the period, amplitude and mean position can also be calculated for each cycle.

To identify the regularity of the breathing pattern, the standard deviations of the amplitudes, mean positions and periods of the breathing cycles in each dataset are calculated. The datasets with large standard deviations are considered 'bad' datasets and indicate irregular breathing patterns to which SMART is not applicable. For the remaining 'good' datasets, individual outlier breathing cycles are singled out using threshold values for period, amplitude and mean positions. These outliers should be excluded from ATT derivation since the treatment will be gated off for those cycles.

Using the remaining N_c 'good' breathing cycles, the period of the ATT is calculated as

$$T_{\mathrm{ATT}} = \frac{1}{N_c}\sum_{j=1}^{N_c} T_j$$

where T_j is the period of the jth cycle. Assume a breathing cycle is represented with N_p phase points. The average tumour position at any phase point of the ATT is given as

$$x_{\mathrm{ATT}}(\varphi_i) = \frac{1}{N_c}\sum_{j=1}^{N_c} x_j(\varphi_i)$$

$$y_{\mathrm{ATT}}(\varphi_i) = \frac{1}{N_c}\sum_{j=1}^{N_c} y_j(\varphi_i)$$

$$z_{\mathrm{ATT}}(\varphi_i) = \frac{1}{N_c}\sum_{j=1}^{N_c} z_j(\varphi_i)$$

$$\varphi_i = \frac{2\pi i}{N_p} \qquad i = 1, 2, \ldots, N_p.$$

Using this method, the resulting ATT characterizes the shape of the tumour trajectory, despite changes in the period, amplitude and mean position from cycle to cycle. Assume a breathing cycle can be fitted as (for simplicity, we only write out x coordinate):

$$x_j(\varphi_i) = A_{x,j} f_x(\varphi_i) + \bar{x}_j$$

where f_x describes the shape of the tumour trajectory. The derived ATT is then

$$x_{\mathrm{ATT}}(\varphi_i) = A_{x,\mathrm{ATT}} f_x(\varphi_i) + \bar{x}_{\mathrm{ATT}}$$

which maintains the trajectory shape with average amplitude and mean position:

$$A_{x,\mathrm{ATT}} = \frac{1}{N_c}\sum_{j=1}^{N_c} A_{x,j}$$

$$\bar{x}_{\mathrm{ATT}} = \frac{1}{N_c}\sum_{j=1}^{N_c} \bar{x}_j.$$

2.3. Simulation of SMART treatment

The treatment process of SMART has been simulated to answer the question of how well does ATT work during free breathing conditions. As part of the simulation, we computed the delivery duty cycle, which represents the effectiveness of the ATT, for various situations that are relevant to a practical SMART treatment.

In photon radiotherapy treatment, tumour motion in the beam's eye view (BEV) usually causes more severe dosimetric errors than the motion along the beam direction. This is simply

Table 1. Analysis results for measured lung tumour trajectory data with maximum peak-to-peak motion greater than 1 cm. The duration (in seconds), average breathing cycle period and amplitude, relative standard deviations of the period and amplitude and the relative standard deviation of the tumour mean position along cranio–caudal direction in every breathing cycle are shown.

Dataset no	Duration (s)	T_{ave} (s)	σ_T/T_{ave} (%)	A_{ave} (mm)	σ_A/A_{ave} (%)	σ_Y/A_{ave} (%)
1	129	2.8	7	10.8	8	4
2	114	2.7	11	10.5	16	9
3	100	3.4	9	7.6	6	5
4	114	3.3	13	13.2	20	12
5	130	4.0	7	12.4	9	5
6	87	3.4	17	13.5	24	12
7	107	3.8	14	12.1	9	4
8	133	3.1	12	11.2	21	25
9	163	3.1	12	12.7	24	25
10	94	3.5	14	22.5	12	15
11	205	3.1	25	19.9	49	38

because the dose distribution of a single photon field has a sharp edge in the BEV while along the depth direction the dose fall-off follows an approximate exponential attenuation curve. In SMART treatment, we only track the 2D tumour motion in the BEV and ignore the motion in beam direction. A more realistic simulation should be done for various beam orientations, only using the BEV projections of ATT and tumour trajectory. However, to simplify the problem, in this work we only simulate SMART treatment at a lateral gantry angle, which gives the worst-case scenario because most lung tumour motion is in the cranial–caudal and anterior–posterior directions.

Assume ε_r and ε_φ are the gating thresholds for position and phase, respectively, $|\Delta\vec{r}|$ is the distance in 2D between the tumour and the radiation beam and $|\Delta\varphi|$ is the phase difference. In the simulation, the radiation beam moves along the ATT while the tumour moves according to measured 3D tumour trajectory data. When $|\Delta\vec{r}| > \varepsilon_r$ and/or $|\Delta\varphi| > \varepsilon_\varphi$, the simulated SMART treatment is gated off, i.e., radiation is turned off and the aperture stops moving. After the synchronization between tumour motion and aperture motion is re-established (i.e., $|\Delta\vec{r}| \leqslant \varepsilon_r$, $|\Delta\varphi| \leqslant \varepsilon_\varphi$), the radiation is turned on again and the aperture starts to move with the tumour. If the phase of the tumour motion is ahead the phase of the beam motion, the beam waits at least one full cycle for the next phase synchronization.

In this study, SMART simulations were performed for various clinically relevant parameters, including different position gating thresholds (2 and 3 mm in distance), different durations of treatment time for one field (10, 30 and 50 s) and various starting exhale phases in the measured 3D trajectory. The phase threshold was set to 180°. Basically in this study the treatment is gated on and off according to the distance between tumour and radiation beam. The phase threshold is only used to make sure that a true synchronization between tumour and beam motion is achieved. The treatment time for one IMRT field depends on the monitor units delivered and the dose rate used. The values used here are representative. The length of the measured trajectory data is usually much longer than the treatment time. Due to the irregularity of the breathing pattern, the calculated duty cycle depends on where in the trajectory data the simulation treatment begins. To get a realistic estimation, the simulation was started at every possible exhale phase. Then the mean value and standard deviation of the duty cycles were calculated.

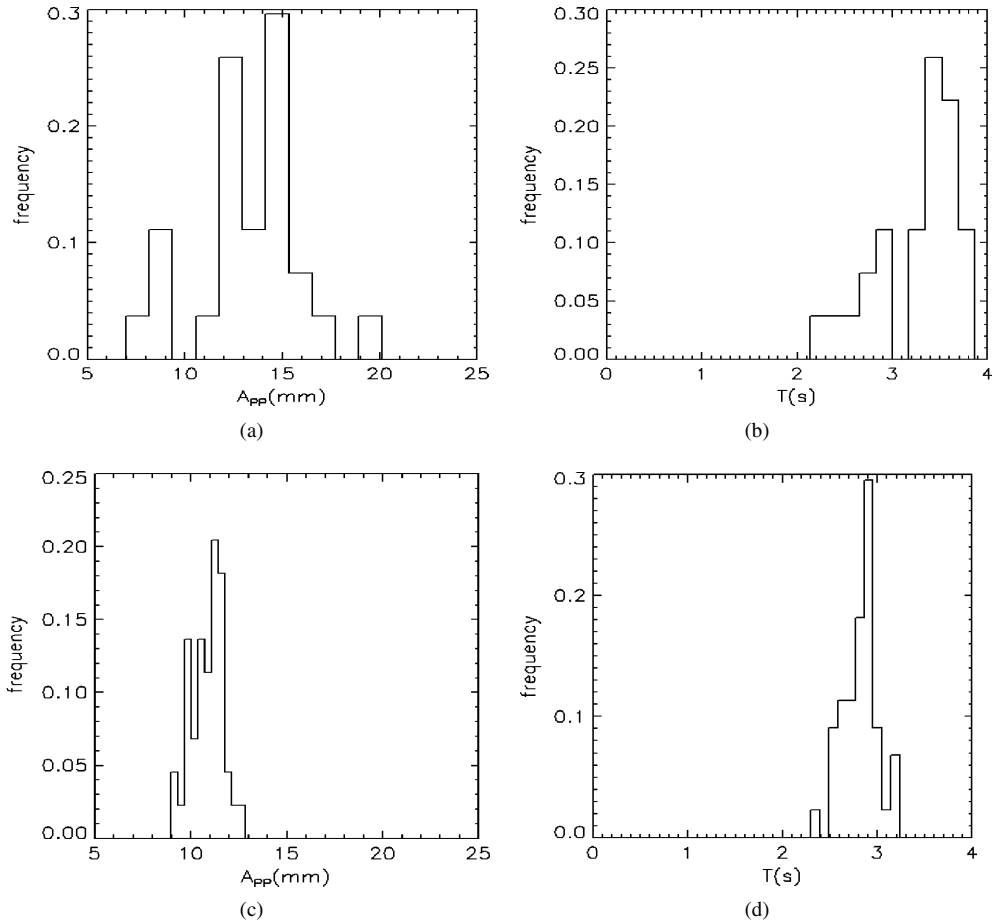

Figure 1. Example of normalized frequency distributions of breathing cycle amplitudes (A_{pp}) and periods (T) for 'bad' and 'good' datasets. The tumour motion depicted in parts (a) and (b) (dataset no 6) has large standard deviations of amplitude and period, due to an irregular breathing pattern, while in parts (c) and (d) (dataset no 1) the smaller standard deviations reveal a regular pattern.

3. Results

Among 41 sets of measured lung tumour trajectory data, there are 11 sets of data with maximum peak-to-peak tumour motions greater than 1 cm and these datasets have been chosen to test SMART. The results of analysis of the breathing pattern regularity of each set are shown in table 1. For each dataset, we present its duration (in seconds), the average breathing cycle period (T_{ave}) and amplitude (A_{ave}), the relative standard deviations of the period (σ_T/T_{ave}) and amplitude (σ_A/A_{ave}), as well as the relative standard deviation of the tumour mean position along the cranial–caudal (y) direction in every breathing cycle (σ_Y/A_{ave}). The duration of these 11 datasets ranges from about 80 s to 200 s, with an average of 125 s. The average period changes from 2.7 s to 4.0 s with a mean value around 3.3 s. One may note that the average amplitude for dataset no 3 is only 7.6 mm; it was selected because the maximum peak-to-peak motion is greater than 10 mm. It is believed that the combination of σ_T/T_{ave}, σ_A/A_{ave} and σ_Y/A_{ave} is a good index for the regularity of the breathing pattern. For dataset nos 1, 3 and 5, all three parameters are smaller than 10% and indicate regular breathing patterns.

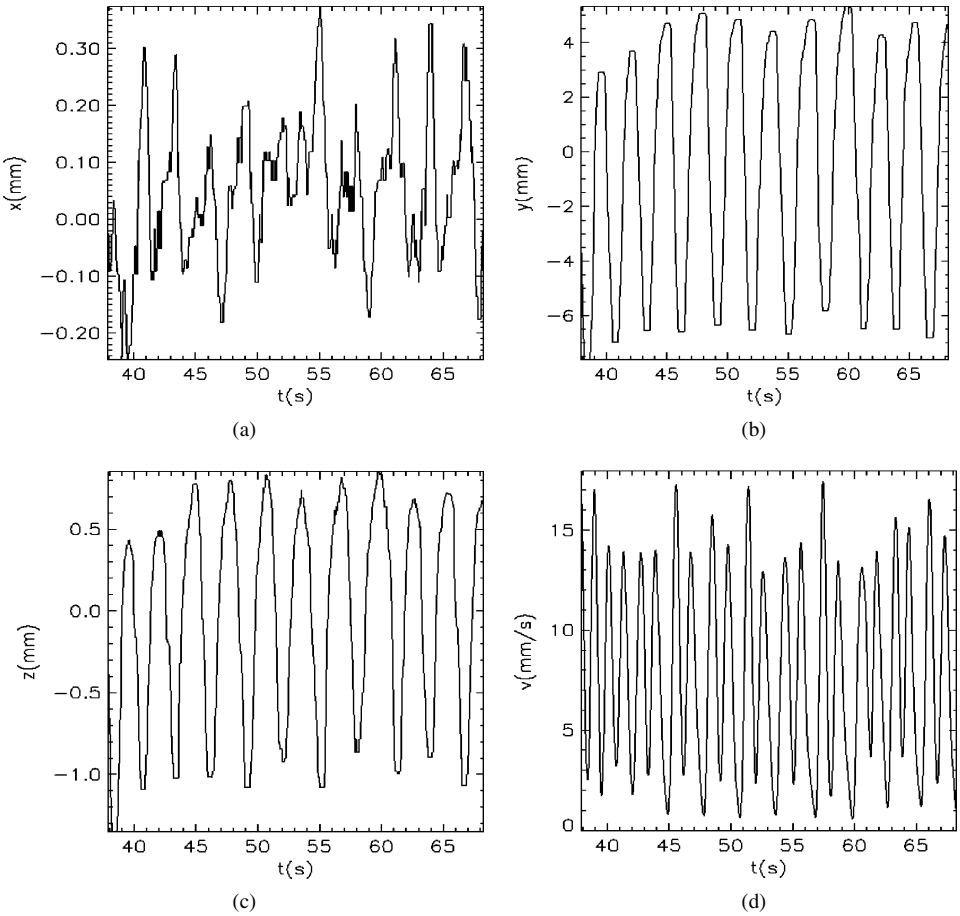

Figure 2. Example of time dependence of lung tumour trajectory (dataset no 1) projected on (a) x (left–right), (b) y (cranial–caudal) and (c) z (anterior–posterior) directions. (d) The velocity of the tumour along its 3D trajectory for the same dataset.

As examples of patients with 'bad' (irregular) and 'good' (regular) breathing patterns, the normalized frequency distributions of breathing cycle amplitudes and periods for dataset nos 1 and 6 are shown in figure 1. From table 1, for dataset no 1, σ_T/T_{ave} and σ_A/A_{ave} are 7% and 8%, respectively, and for dataset no 6, 17% and 24%, respectively. Apparently, dataset no 6 does not have a regular breathing pattern and the ATT will not be a valid concept for this case.

In figure 2, we present an example (dataset no 1) of the measured tumour trajectory projected along the main directions and the corresponding velocity curve. For this dataset, as for many lung cancer patients, the tumour motion along y (cranial–caudal) direction has the largest amplitude (about 1 cm from peak to peak), while the motion along the other two (left–right and anterior–posterior) is negligible. The local minima in the velocity curve of the tumour along its trajectory (depicted in figure 2(d)) correspond to the inhale and exhale breathing phases. The calculated ATT curve projected along three main directions $([x(\varphi_i), y(\varphi_i), z(\varphi_i)])$ for the same dataset are shown in figure 3. The error bars are the standard deviations of the measured tumour positions at a given breathing phase. It can be seen that for this patient the ATT concept is valid, and the measured trajectory data scatter around the ATT curve with relatively small deviations.

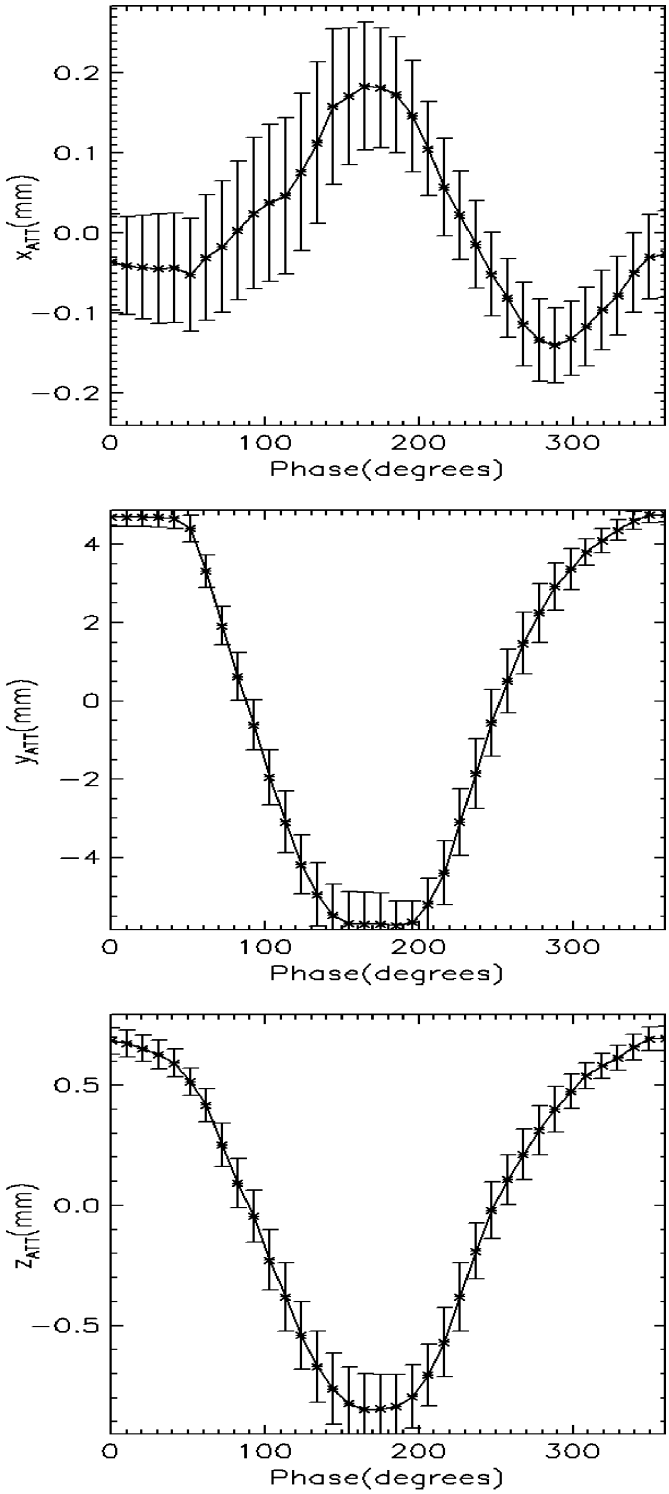

Figure 3. Derived average tumour trajectories (ATT) x_{ATT}, y_{ATT}, z_{ATT} for dataset no 1. The error bars represent the standard deviations of the measured tumour positions at a given breathing phase.

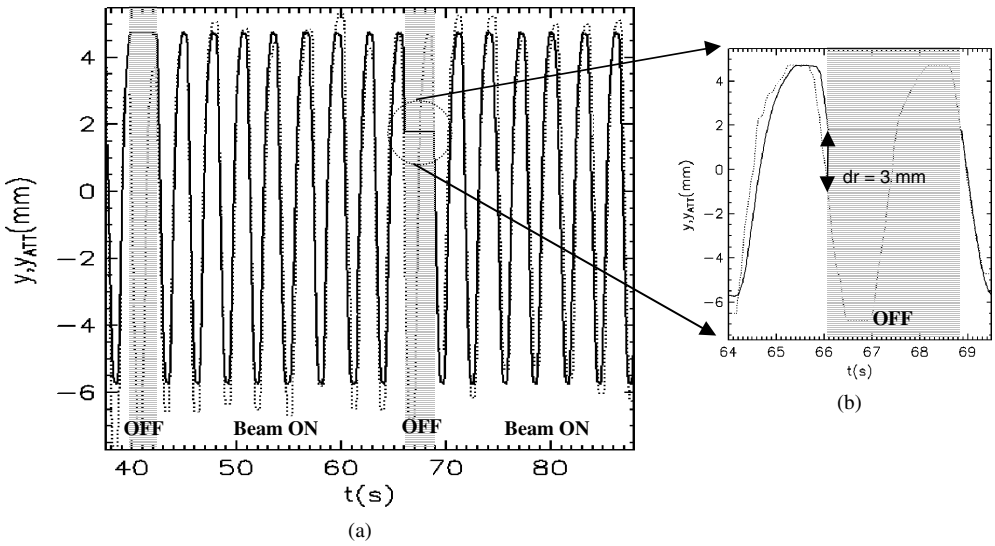

Figure 4. (a) Simulation of a SMART treatment using the calculated ATT. The tumour position y is depicted by the dotted line, while the continuous line represent the beam position, which moves along y_{ATT}. The gating threshold is 3 mm. (b) Inset showing details about how the treatment is gated off and on again. Note that dr represents the 2D distance, i.e., $\mathrm{d}r = \sqrt{\mathrm{d}y^2 + \mathrm{d}z^2}$.

The ATT curves derived from the measured patient data were used to simulate SMART treatment to estimate the delivery efficiency. As an example, figure 4 shows the simulated movement of tumour and radiation beam along the cranial–caudal direction, for dataset no 1. In the simulation, the radiation beam moves according to the ATT and the tumour moves based on the measured trajectory data. The gating threshold used here is 3 mm for the position and 180° for the phase. At $t = 40$ s, the difference between the tumour and beam positions exceeds the tolerance and, therefore, the treatment is gated off. From figure 4, we see that the radiation beam stops moving and waits for the tumour to return. At $t = 42$ s, the synchronization between tumour motion and beam motion is re-established and the treatment continues until $t = 66$ s when the tolerance is exceeded again (see figure 4(b)). The treatment is resumed at $t = 69$ s. It can be seen that for this dataset, the treatment efficiency is high, due to the regular breathing pattern as seen in table 1.

Table 2 shows a summary of the simulated SMART treatment results for the first five datasets from table 1. The mean duty cycle associated with the standard deviation is shown for each combination of the gating threshold and treatment time. The standard deviation was calculated by varying the treatment starting point at every possible exhale phase in the measured trajectory. It is noticed that the duty cycle for dataset nos 1, 3 and 5 are higher than 60% when the one-field treatment time is greater than 30 s. This is consistent with our previous analysis based on table 1. Additionally, dataset no 2 also presents good duty cycle (around 60% for 30 and 50 s delivery time). Therefore, out of 11 datasets, a total of four have a reasonable duty cycle when treated with SMART.

4. Discussion and conclusions

ATT is the basis of SMART, a new technique for treating moving tumours. This paper has proposed the concept of ATT and tried to answer two questions related to ATT: (1) how can

Table 2. Summary of simulated SMART treament results obtained for different position gating thresholds dr (2, 3 mm), different lengths of treatment time for a single field (10, 30, 50 s) and various starting exhale phases in the measured trajectory.

			SMART duty cycle (%)		
			Treatment time (s)		
Dataset no	A_{max} (mm)	dr (mm)	10	30	50
1	13	2	43 ± 20	49 ± 12	52 ± 6
		3	56 ± 15	71 ± 10	76 ± 6
2	13	2	44 ± 10	45 ± 14	46 ± 7
		3	49 ± 19	59 ± 16	61 ± 7
3	11	2	52 ± 19	66 ± 14	67 ± 9
		3	63 ± 15	82 ± 11	83 ± 9
4	20	2	23 ± 22	23 ± 17	21 ± 7
		3	45 ± 24	48 ± 22	49 ± 9
5	15	2	29 ± 19	34 ± 11	34 ± 11
		3	47 ± 18	60 ± 11	64 ± 8

the ATT for an individual patient be derived from tumour trajectory data measured at the treatment planning/simulation stage? (2) How well does ATT work for lung cancer patients under free breathing? In other words, do we need breath coaching/control to make SMART efficient enough?

For tumours with small motion amplitudes, there is less need to use SMART and thus to derive ATT. In clinical use of SMART, choosing a proper cut-off value for tumour motion amplitude is an important issue which has to be addressed carefully. In this paper, we chose arbitrarily the maximum peak-to-peak motion of 1 cm as the cut-off value. Eleven of 41 available measured tumour trajectory datasets satisfy this criterion. That means, based on this criterion, about a quarter of lung patients can potentially benefit from SMART treatment. However, this conclusion is only qualitative, because not only is the cut-off value arbitrarily chosen, but also the study pool may not be large enough. Furthermore, the percentage of patients with large tumour motions may be different for different population groups. For example, larger persons have large lung capacities and, therefore, will most likely have larger lung tumour motions.

The 11 sets of data were first analysed and three parameters, i.e., relative standard deviations of the period (σ_T/T_{ave}), amplitude (σ_A/A_{ave}) and mean position (σ_Y/A_{ave}), were derived for each dataset. These three parameters can be used as useful indices to screen out datasets with irregular patterns.

A simple method has been developed to derive the ATT. This method conserves the tumour trajectory shape, no matter how much the motion period, amplitude and mean position differ between breathing cycles. The derived ATT is the average tumour position at each phase of a breathing cycle. If the breathing cycle phase at a specific time during the treatment can be estimated, then the tumour position can be predicted using the ATT.

The simulation of the SMART treatment was performed using the derived ATT. In the simulation, the tumour moves according to the measured trajectory and the beam moves along ATT. Ideally, if we had multiple sets of trajectory data for various treatment fractions for the same patient, we could have used one set of data to derive ATT and used the others for simulation. This way, the simulation is more realistic. However, due to the small size of the data pool, we decided to treat each dataset independently and to use the same dataset

for both ATT derivation and SMART simulation. Therefore, the correlation between ATT and the testing data is stronger than that if we had used different datasets for simulation, and the calculated duty cycle may be overestimated. However, the simulation was performed in the lateral beam orientation where the tumour motion is the largest in the beam's eye view and represents the worst-case scenario. The result is the underestimation of duty cycle which mitigates the overestimation due to the correlation between ATT derivation and SMART simulation. After all, the calculated duty cycle values are used in this work in a relative and qualitative way.

The simulation was done for 11 datasets with maximum peak-to-peak motion greater than 1 cm. Reasonable treatment efficiency was achieved for about one third of cases (4 out of 11 datasets). It is found that in general the SMART treatment is not much more efficient than respiratory gating if the patient breathes freely. This is solely due to the irregularity of patient's breathing pattern during free breathing.

SMART is applicable only if a patient's breathing cycle does not change over the course of radiotherapy treatment. However, a patient's breathing pattern could change from fraction to fraction. An alternative would be to calculate the ATT of a patient on more than one occasion by having several simulations throughout the treatment course. Or more practically, breath coaching can be used to maintain the same breathing pattern for every fraction.

The regularity of the breathing pattern during one treatment and from fraction to fraction should be improved if breath coaching/control techniques are used. This will be investigated in our future research. We expect the SMART treatment to be suitable and have high efficiency for patients with regular breathing patterns.

Acknowledgments

We acknowledge stimulating discussions with Dr Ross Berbeco, Dr Gregory Sharp and Mr Khaled Jarrah. This work was supported by the Whitaker Foundation Grant RG-01–0175.

References

Adler J R Jr, Murphy M J, Chang S D and Hancock S L 1999 Image-guided robotic radiosurgery *Neurosurgery* **44** 1299–306 (discussion 1297–1306)

Ford E C, Mageras G S, Yorke Y, Rosenzweig K E, Wagman R and Ling C C 2002 Evaluation of respiratory movement during gated radiotherapy using film and electronic portal imaging *Int. J. Radiat. Oncol. Biol. Phys.* **52** 522–31

Hanley J *et al* 1999 Deep inspiration breath-hold technique for lung tumors: The potential value of target immobilization and reduced lung density in dose escalation *Int. J. Radiat. Oncol. Biol. Phys.* **45** 603–11

Jiang S B *et al* 2000 Compensating for tumor motion using a computer-controlled multi-leaf collimator in radiation therapy *Application for The Whitaker Foundation Biomedical Engineering Research Grants*

Keal P J, Kini V R, Vedam S S and Mohan R 2001 Motion adaptative x-ray therapy: a feasibility study *Phys. Med. Biol.* **46** 1–10

Kitamura K *et al* 2002 Three-dimensional intrafractional movement of prostate measured during real-time tumor-tracking radiotherapy in supine and prone treatment positions *Int. J. Radiat. Oncol. Biol. Phys.* **53** 1117–23

Kubo H D and Hill B C 1996 Respiration gated radiotherapy treatment: a technical study *Phys. Med. Biol.* **41** 83–91

Kubo H D, Len P M, Minohara S and Mostafavi H 2000 Breathing-synchronized radiotherapy program at the University of California Davis Cancer Center *Med. Phys.* **27** 346–53

Kubo H D and Wang L 2000 Compatibility of Varian 2100C gated operations with enhanced dynamic wedge and IMRT dose delivery *Med. Phys.* **27** 1732–38

Mah D, Hanley J, Rosenzweig K E, Yorke E, Braban L, Ling C C, Leibel S A and Mageras G 2000 Technical aspects of the deep inspiration breath-hold technique in the treatment of thoracic cancer *Int. J. Radiat. Oncol. Biol. Phys.* **48** 1175–85

Minohara S, Kanai T, Endo M, Noda K and Kanazawa M 2000 Respiratory gated irradiation system for heavy-ion radiotherapy *Int. J. Radiat. Oncol. Biol. Phys.* **47** 1097–103

Murphy M, Martin D, Whyte R, Hai J, Ozhasoglu C and Le Q 2002 The effectiveness of breath-holding to stabilize lung and pancreas tumors during radiosurgery *Int. J. Radiat. Oncol. Biol. Phys.* **53** 475–82

Ohara K, Okumura T, Akisada T, Inada T, Mori T, Yokota H and Calguas M B 1989 Irradiation synchronized with respiration gate *Int. J. Radiat. Oncol. Biol. Phys.* **17** 853–7

Ozhasoglu C and Murphy M J 2002 Issues in respiratory motion compensation during external-beam radiotherapy *Int. J. Radiat. Oncol. Biol. Phys.* **52** 1389–99

Ozhasoglu C, Murphy M J, Glosser G, Bodduluri M, Schweikard A, Forster K M, Martin D P and Adler J R 2000 Real-time tracking of the tumor volume in precision radiotherapy and body radiosurgery—a novel approach to compensate for respiratory motion *Proc. 14th Int. Conf. on Computer Assisted Radiology and Surgery (CARS) (San Francisco, CA, USA)*

Ramsey C R, Cordrey I L and Oliver A L 1999a A comparison of beam characteristics for gated and nongated clinical x-ray beams *Med. Phys.* **26** 2086–91

Ramsey C R, Scaperoth D, Arwood D and Oliver A L 1999b Clinical efficacy of respiratory gated conformal radiation therapy *Med. Dosim.* **24** 115–9

Rosenzweig K E *et al* 2000 The deep inspiration breath-hold technique in the treatment of inoperable non-small-cell lung cancer *Int. J. Radiat. Oncol. Biol. Phys.* **48** 81–7

Schweikard A, Glosser G, Bodduluri M, Murphy M J and Adler J R 2000 Robotic motion compensation for respiratory movement during radiosurgery *Comput. Aided Surg.* **5** 263–77

Seppenwoolde Y *et al* 2002 Precise and real-time measurement of 3D tumor motion in lung due to breathing and heartbeat, measured during radiotherapy *Int. J. Radiat. Oncol. Biol. Phys.* **53** 822–34

Shirato H *et al* 2000 Physical aspects of a real-time tumor-tracking system for gated radiotherapy *Int. J. Radiat. Oncol. Biol. Phys.* **48** 1187–95

Stromberg J S, Sharpe M B, Kim L H, Kini V R, Jaffray D A, Martinez A A and Wong J W 2000 Active breathing control (ABC) for Hodgkin's disease: reduction in normal tissue irradiation with deep inspiration and implications for treatment *Int. J. Radiat. Oncol. Biol. Phys.* **48** 797–806

Suit H D, Becht J, Leong J, Stracher M, Wood W C, Verhey L and Goitein M 1988 Potential for improvement in radiation therapy *Int. J. Radiat. Oncol. Biol. Phys.* **14** 777–86

Wong J W, Sharpe M B, Jaffray D A, Kini V R, Robertson J S, Stromberg J S and Martinez A A 1999 The use of active breathing control (ABC) to reduce margin for breathing motion *Int. J. Radiat. Oncol. Biol. Phys.* **44** 911–9

Vedam S S, Keall P J, Kini V R and Mohan R 2001 Determining parameters for respiration-gated radiotherapy *Med. Phys.* **28** 2139–46